Theoretical investigation on the addition reaction of the germylenoid $H_2GeLiCl$ with acetone

Xiaolin ZHANG, Bingfei YAN, Wenzuo LI*

School of Chemistry and Chemical Engineering, Yantai University, Yantai, P. R. China

ORCID iD numbers of all authors:

Xiaolin ZHANG: 0000-0003-3980-5853

Bingfei YAN: 0000-0001-6560-0005

Wenzuo LI: 0000-0002-1630-619X

Abstract: In this work, theoretical calculations were performed on the addition reaction of the germylenoid $H_2GeLiCl$ with acetone. The DFT M06-2X method was used to optimize the geometries of the whole stationary points on the potential energy surfaces and the QCISD method to calculate the single-point energy. The results reveal that the addition reaction of $H_2GeLiCl$ with acetone firstly generates an oxagermacyclopropane *c*-$H_2GeOC(CH_3)_2$ and then *c*-$H_2GeOC(CH_3)_2$ further reacts with acetone along two possible pathways, pathway I and pathway II, in which the 2,4-dioxagermolane is formed at the end of pathway I and 2,5-dioxagermolane is formed at the end of pathway II, respectively. According to the calculated barrier heights, we can deduce that the pathway I is more favorable than pathway II. The computational results suggest that this reaction model can provide new inspiration for the synthesis of heterocyclic germanium compounds.

* Correspondence: liwenzuo2004@126.com

Key words: $H_2GeLiCl$, acetone, addition reaction, spiro-Ge-heterocyclic

1. Introduction

For recent years, germylene and its derivatives have been well studied as a bioactivator in medicine. Germylenoid is a derivative of germylene. Since Lei and Gaspar [1] firstly pointed out that there may exist an intermediate named germylenoid in the reaction of dichlorodimethylgermane with lithium in the presence of substituted 1,3-dienes in 1991, both theoretical and experimental research on germylenoid have been going on for more than 20 years. In 2000, Ichinohe et al. [2] proved that an active germylenoid intermediate *t*-$Bu_3SiGeCl_2Na$ played an important role in the reaction of *t*-Bu_3SiNa with $GeCl_2$ · dioxane. In 2006, Tokitoh et al. [3, 4] pointed out that an important intermediate in the addition reaction of 1,2,4,5-tetrabromobenzene with dilithiogermane Tbt(Dip)$GeLi_2$ was germylenoid Tbt(Dip)GeLiBr. In 2012, Fillipou et al. [5] firstly synthesized the zwitterionic germylidene complexes and they believed a germylenoid was one of the reactants in the reaction. There was no one stable germylenoids being prepared experimentally until Sasamori et al. [6] firstly synthesized a stable germylenoid successfully in 2016. A chlorogermylenoid (Fc*$GeCl_2Li$) that includes 2,5-bis(3,5-*di*-*t*-butylphenyl) ferrocenyl (Fc*) group was generated in their groundbreaking work and the specific structure and ambident reactivity of this chlorogermylenoid were investigated. With the development of the experimental works about germylenoids, more attentions

have been paid to theoretical researches [7–32]. In 1999, Qiu et al. [7] firstly studied the germylenoid H_2GeLiF by *ab initio* quantum calculations method. By analyzing structures and the solvent effect in different solvents of the germylenoid H_2GeLiF, Ma et al. [8] obtained four possible stable equilibrium structures in the gas phase in 2007. In 2006, Li et al. [9] firstly came up with this concept for unsaturated germylenoid H_2C=GeNaF. In 2008, Tan [10] systematically investigated the geometries and isomerization of the germylenoid HN=GeNaF and discussed the insertion reactions with R–H (R = F, OH, NH_2, CH_3), and the study came to a conclusion that the relative reactivity of reactants is as follows: H–F > H–OH > H–NH_2 > H–CH_3. The structures and properties of other different germylenoids such as H_2GeLiF [11, 12], $H_2GeFMgF$ [13], $H_2GeZnCl_2$ [14], HP=GeLiF [15], $H_2GeAlCl_3$ [16], and so on, were investigated using theoretical methods. The different reactions such as insertion, elimination, substitution and addition reactions [11–32] of germylenoids were also analyzed by theoretical calculations. These works provide a lot of useful information for the correct understanding of the structure, properties and reactivity of germylenoid compounds. However, few studies have been done on the addition reactions of germylenoid. Only the addition reactions of some germylenoid with ethylene [13–16,26–31] and formaldehyde [32] have been reported in the literature. Recently, we have calculated the addition reaction of $H_2GeLiCl$ with acetone and found that the product is a heterocyclic germanium compound, which provides new inspiration for the synthesis of new germanium-containing compounds.

2. Theoretical methods

The relevant calculation details have been depicted in previous research [16]. The instrument that caused the calculation to be implemented was Gaussian 09 series of programs [33]. The geometries of the whole stationary points were optimized by using the method of density functional theory (DFT) M06-2X [34, 35] and 6-311+G (d, p) [36] basis set (BSI). The vibrational frequency was calculated by the same method in order to confirm the minima or saddle points of structures and obtain zero-point energies (ZPEs). The mechanism of the addition reaction pathways was proved by using the IRC [37] analysis to probe every transition state connected with the corresponding stationary points correctly. The single-point computations were carried out using QCISD [38, 39] method with 6-311++G (d, p) basis set (BSII). The given relative energies in this paper were calculated by QCISD/BSII//M06-2X/BSI level and including the M06-2X/BSI calculated ZPEs (without scale) corrections. The molecular electrostatic potentials (MEPs) for the reactants were also calculated at M06-2X/BSI level.

3. Results and discussions

The previous calculations [2, 11, 12] proved that germylenoid $H_2GeLiCl$ has three equilibrium structures, and the most stable configuration of them is the *p*-complex. That is to say, the *p*-complex structure of $H_2GeLiCl$ is obviously the target when we investigated the addition reaction of germylenoid $H_2GeLiCl$ (R1) and acetone CH_3COCH_3 (R2).

There are two steps in the addition reaction of $H_2GeLiCl$ with acetone according to the calculation results. In the first step, an oxagermacyclopropane (*c*-$H_2GeOC(CH_3)_2$,

marked as P) can be generated. In the second step, P can further react with acetone CH_3COCH_3 in two possible pathways. The M06-2X/BSI calculated MEPs for R1, R2 and P were shown in Scheme 1. From Scheme 1 it can be seen that there is a positive electrostatic potential region around the Ge atom in R1 and a negative electrostatic potential region around the O atom in R2. The interaction of these two regions will lead to the first step of the reaction of R1 and R2. Interestingly, there are two positive electrostatic potential regions around the Ge atom in P. When the O atoms in acetone approach different positive electrostatic potential regions of P, different reaction pathways (path I and II) will occur. These two steps and two different pathways will be illustrated in detail.

3.1. Step 1 of the addition reaction of $H_2GeLiCl$ with acetone

The reaction equation for the first step of the reaction of germylenoid $H_2GeLiCl$ with CH_3COCH_3 is depicted as follows:

$$H_2GeLiCl\ (R1) + CH_3COCH_3\ (R2) \rightarrow LiCl + \textit{c}\text{-}H_2GeOC(CH_3)_2\ (P)$$

Based on the computation results, we found that along the potential energy surface there is one precursor complex (Q), one transition state (TS), and one intermediate (IM). The geometries of the stationary points which calculated at the M06-2X/BSI level are shown in Figure 1, and their relative energies are shown in Figure 2. The calculated structure coordinates of reactants, intermediates, transition states and products were shown in Supporting information.

One precursor complex Q will be formed when R1 approaches R2 as shown in

Figure 1. The distances of O-Ge and C-Ge are 0.267 and 0.355 nm respectively and the C-O-Ge angle is 129.4 degrees. These facts indicated the interaction between R1 and R2 is weak and the reaction will proceed further. As shown in Figure 2, the relative energy of Q is -13.69 kJ/mol.

Due to the rotation of acetone (<90º), the distance of O-Ge and C-Ge are becoming shorter and the C-O-Ge angle is becoming smaller, a transition state (TS) is formed. As shown in Figure 1, in TS the distance of O-Ge and C-Ge are 0.212 and 0.201 nm respectively, and the C-O-Ge angle is only 70.5 degrees. The IRC results show that TS is correctly in the middle of Q and intermediate IM. The imaginary frequency of TS is 207.0i cm^{-1}. The relative energy of TS is 77.56 kJ/mol, consequently, the barrier height is 91.25 kJ/mol.

As reaction goes on, the intermediate IM will be formed after TS, and it can be regarded as the complex of the last products LiCl and *c*-$H_2GeOC(CH_3)_2$ (P). As shown in Figure 1, in IM the distances of O-Ge and C-Ge of IM further decrease to 0.187 and 0.192 nm respectively, and the angle of C-O-Ge is 69.4 degrees, which indicates the formation of O-Ge and C-Ge bonds. As shown in Figure 2, the relative energy of IM is 68.27 kJ/mol.

The reaction of $H_2GeLiCl$ (R1) and CH_3COCH_3 (R2) resulted in the formation of LiCl and *c*-$H_2GeOC(CH_3)_2$ (P) in the first step. The relative energies of the products (LiCl +*c*-$H_2GeOC(CH_3)_2$) is 99.17 kJ/mol. It can be seen that the addition reaction of $H_2GeLiCl$ with acetone is endothermic in the first step.

3.2. Step 2 of the addition reaction of $H_2GeLiCl$ with acetone

The M06-2X/BSI calculations indicate that there are two possible pathways (path I and II) in the reaction of *c*-$H_2GeOC(CH_3)_2$ and CH_3COCH_3. The Ge atom of *c*-$H_2GeOC(CH_3)_2$ approaches the O atom of CH_3COCH_3 in the path I and path II and then interacts with each other. But the interaction from different directions results in different transition states and ultimate products. In path I, the O1-Ge bond of *c*-$H_2GeOC(CH_3)_2$ and the O2-C2 bond of CH_3COCH_3 are spatially close in a parallel manner, and then the O1-Ge bond of *c*-$H_2GeOC(CH_3)_2$ is broken, with the Ge atom approaching and interacting with the O2 atom of CH_3COCH_3, at the same time, the O1 atom of *c*-$H_2GeOC(CH_3)_2$ approaches and interacts with the C2 atom of CH_3COCH_3 to form the product 2,4-dioxagermolane (P1). However, in path II, the O2-C2 bond of CH_3COCH_3 is not parallel to the O1-Ge bond of *c*-$H_2GeOC(CH_3)_2$ but approaching the C1-Ge bond of *c*-$H_2GeOC(CH_3)_2$ in an almost parallel manner. After the C1-Ge bond of *c*-$H_2GeOC(CH_3)_2$ is broken, the Ge atom approaches and interacts with the O2 atom of CH_3COCH_3 and the C1 atom of *c*-$H_2GeOC(CH_3)_2$ approaches and interacts with the C2 atom of CH_3COCH_3 causing the formation the product 2,5-dioxagermolane (P2). As shown in Figure 3, TS1 is the transition state of path I, of which unique imaginary frequency is 231.82i cm^{-1} calculated by M06-2X/BSI. The relative energy of TS1 is 56.94 kJ/mol as depicted in Figure 4, which is the barrier height of path I. A spiro-Ge-heterocyclic product(P1), 2,4-dioxagermolane, is formed at the end of path I, and the relative energies of P1 is -147.84 kJ/mol.

In path II, TS2 is the transition state as shown in Figure 3. The unique imaginary frequency of TS2 is 406.6i cm^{-1} calculated by M06-2X/BSI. The relative energy of TS2

is 134.35 kJ/mol (in Figure 4), which is the barrier height of path II. At the end of path II, the other spiro-Ge-heterocyclic product (P2) forms, which is the 2,5-dioxagermolane. The relative energy of P2 is -218.88 kJ/mol.

We can find that path I and II are both exothermic. The barrier height of path I is about 77.41 kJ/mol lower than path II which can be concluded from Figure 4. Then we can draw a conclusion that the path I is more favorable dynamically.

3.3. The mechanism of addition reactions

For studying the addition reaction pathway, the IRC analysis was carried out on the basis of the TS, TS1 and TS2 to study the interactions of the step 1 and the step 2 respectively in the addition reaction.

We took the first step as an example. The total energy (E) of the reactants and the bond lengths of C-Ge and O-Ge are shown in Figure 5 along the reaction pathway. With the reaction coordinates rises from -5.0 to 0.0, the total energy (E) increases rapidly and reaches a peak. Also, the bond lengths of C-Ge and O-Ge gradually decrease to a stable value, which indicates the formation of C-Ge and O-Ge bonds. Consequently, TS connects Q and IM correctly. In the two paths of the step 2, the results of IRC calculations of the TS1 and TS2 are also shown in Figure 5 and both of them are correct.

4. Conclusions

By using the DFT M06-2X and QCISD methods, firstly we studied the addition reaction of the germylenoid $H_2GeLiCl$ with acetone. The geometry optimizations were carried out

at M06-2X/6-311+G (d, p) level and the single-point energies were computed at the QCISD/6-311++G (d, p) level in sequence. The results reveal that there are two ways existing for the reaction of $H_2GeLiCl$ and CH_3COCH_3, and different products are formed: 2,4-dioxagermolane (P1) and 2,5-dioxagermolane (P2), respectively. The process can be viewed as a two-step reaction and the step 1 is the same for two products. In step 1, $H_2GeLiCl$ and acetone react and oxagermacyclopropane (P) is formed by an addition reaction. There is a precursor complex, a transition state and an intermediate existing in step I along the potential energy surface. In step 2, there is a continuous reaction of product oxagermacyclopropane (P) with acetone, and the different bond-forming ways of them lead to the formation of different spiro-Ge-heterocyclic products. There are two possible pathways (I and II), which finally form spiro-Ge-heterocyclic products 2,4-dioxagermolane (P1) and 2,5-dioxagermolane (P2), respectively. The barrier height of path I is 56.94 kJ/mol while the barrier height of path II is 134.35 kJ/mol, which means the path I favors thermodynamically. Therefore, it can concluded that the dominant channel of the addition reaction of $H_2GeLiCl$ and CH_3COCH_3 is that firstly R1 + R2→ P and then P + R2 → P1. We are confident that this work will provide a new inspiration for the synthesis of new germanium-containing compounds.

Acknowledgements

The authors gratefully acknowledge financial support from the Natural Science Foundation of Shandong Province (No. ZR2016BM23).

References

1. Lei DQ, Gaspar PP. Sonochemical synthesis of 1,1-dimethyl-1-germacyclopent-3-enes and the extrusion of dimethylgermylene upon their pyrolysis. Polyhedron 1991; 10 (11): 1221-1225. doi: 10.1016/S0277-5387(00)86098-2
2. Ichinohe M, Sekiyama H, Fukaya N, Sekiguchi A. On the role of cis, trans-(*t*-$Bu_3SiGeCl)_3$ in the reaction of $GeCl_2$, dioxane with tri-*tert*-butylsilylsodium: evidence for existence of digermanylsodium *t*-$Bu_3SiGe(Cl)_2Ge(Cl)(Na)Si$*t*-$Bu_3$ and digermene *t*-$Bu_3Si(Cl)Ge{=}Ge(Cl)Si$*t*-Bu_3. Journal of the American Chemical Society 2000; 122 (28): 6781-6782. doi: 10.1021/ja000057l
3. Sasamori T, Tokitoh N. Synthesis and characterization of two isomers of 14π-electron germaaromatics: kinetically stabilized 9-germaanthracene and 9-germaphenanthrene. Organometallics 2006; 25 (15): 3522-3532. doi: 10.1021/om060371+
4. Tajama T, Sasamori T, Takeda N, Tokitoh N, Yoshida K, et al. Synthesis of bis(germacyclopropa) benzenes and Structures of their annelated benzene rings. Organometallics 2006; 25 (1): 230-235. doi: 10.1021/om0507629
5. Filippou AC, Stumpf KW, Chernov O, Schnakenburg G. Metal activation of a germylenoid, a new approach to metal-germanium triple bonds: synthesis and reactions of the germylidyne complexes $[Cp(CO)_2M{\equiv}Ge{-}C(SiMe_3)_3]$ (M = Mo, W). Organometallics 2012; 31 (3): 748-755. doi: 10.1021/om201176n
6. Suzuki Y, Sasamori T, Guo JD, Nagase S, Tokitoh N. Isolation and ambident reactivity of a chlorogermylenoid. Chemistry-A European Journal 2016; 22 (39): 13784-13788. doi: 10.1002/chem.201602601

7. Qiu HY, Ma WY, Li GB, Deng CH. The isomeric structures of H_2GeLiF, the prototype germylenoid. Chinese Chemical Letters 1999; 10 (6): 511-514.
8. Ma WY, Zhu YF, Zhou JH, Fang YZ. Solvent effect on the structures and isomerizationof germylenoid GeH_2LiF. Journal of Molecular Structure-Theochem 2007; 817 (1-3): 77-81. doi: 10.1016/j.theochem.2007.04.023
9. Li WZ, Cheng JB, Gong BA, Xiao CP. DFT study on the unsaturated germylenoid H_2C=GeNaF. Journal of Organometallic Chemistry 2006; 691 (26): 5984-5987. doi: 10.1016/j.jorganchem.2006.09.028
10. Tan XJ, Wang WH, Li P, Wang QF, Zheng GX, Liu F. Theoretical studies on the imine germylenoid HN=GeNaF and its insertion reaction with R–H (R = F, OH, NH_2, CH_3). Journal of Organometallic Chemistry 2008; 693 (3): 475-482. doi: 10.1016/j.jorganchem.2007.11.019
11. Li WZ, Liu T, Cheng JB, Li QZ, Gong BA. Theoretical investigation on H_2 elimination reactions of germylenoid H_2GeLiF with RH (R = F, OH, and NH_2). Journal of Organometallic Chemistry 2010; 695 (6): 909-912. doi: 10.1016/j.jorganchem.2010.01.016
12. Li WZ, Yan BF, Li QZ, Cheng JB. The insertion reactions of the germylenoid H_2GeLiF with CH_3X (X=F, Cl, Br). Journal of Organometallic Chemistry 2013; 724 (15): 163-166. doi: 10.1016/j.jorganchem.2012.11.012
13. Zhang MX, Yan BF, Li WZ, Li QZ, Cheng JB. Theoretical prediction on the addition reaction of germylenoid $H_2GeFMgF$ with ethylene. Journal of Theoretical and Computational Chemistry 2016; 15 (3): 1650022. doi:

10.1142/S021963361650022X

14. Zhang MX, Yan BF, Li WZ, Li QZ, Cheng JB. Structures of the germylenoid $H_2GeZnCl_2$ and its addition reactions with ethylene. Structural Chemistry 2016; 27 (6): 1819-1829. doi: 10.1007/s11224-016-0802-1
15. Yan BF, Yuan TM, Li WZ, Li QZ, Cheng JB. Structures of the phosphinidene germylenoid HP=GeLiF and its cycloaddition reaction with ethylene. Structural Chemistry 2018; 29 (6): 1647-1653. doi: 10.1007/s11224-018-1142-0
16. Zhang MX, Li WZ, Li QZ, Cheng JB. The addition reactions of germylenoid $H_2GeAlCl_3$ with ethylene: a theoretical investigation. Journal of Molecular Modeling 2017; 23 (7): 199. doi: 10.1007/s00894-017-3375-z
17. Li WZ, Cheng JB, Li QZ, Gong BA, Sun JZ. Theoretical investigation on structures and isomerizations of the aluminumchlorogermylenoid $H_2GeClAlCl_2$. Journal of Organometallic Chemistry 2009; 694 (18): 2898-2901. doi: 10.1016/j.jorganchem.2009.04.023
18. Qi YH, Geng B, Chen ZH. The structures and stability of pentacoordinate germylenoid $PhCH_2(NH_2)CH_3GeLiF$. Structural Chemistry 2011; 22 (4): 917-924. doi: 10.1007/s11224-011-9779-y
19. Li WZ, Cao QZ, Pei YW, Li R, Zhu HJ, et al. Theoretical study on germylenoid $H_2GeFBeF$. Structural Chemistry 2012; 23 (3): 867-871. doi: 10.1007/s11224-011-9933-6
20. Yan BF; Li WZ, Xiao CP, Li QZ; Cheng JB. A new reaction mode of germanium-silicon bond formation: insertion reactions of H_2GeLiF with SiH_3X (X=F, Cl, Br).

Journal of Molecular Modeling 2013; 19 (10): 4537-4543. doi: 10.1007/s00894-013-1970-1

21. Xiao CP, Li WZ, Li QZ, Cheng JB. Substitution reactions of $H_2GeFBeF$ with RH (R = F, OH, NH_2): a theoretical study. Russian Journal of Physical Chemistry A 2014; 88 (7): 1097-1102. doi: 10.1134/S0036024414070103
22. Yan BF, Li WZ, Xiao CP, Liu ZB, Li QZ, et al. New insights into the insertion reactions of germylenoid H_2GeLiF with RH (R=F, OH, NH_2). Journal of Molecular Modeling 2015; 21 (4): 68. doi: 10.1007/s00894-015-2626-0
23. Zhang MX, Zhang MJ, Li WZ, Li QZ, Cheng JB. Structure of $H_2GeFMgF$ and its insertionreactions with RH (R=F, OH, NH_2). Journal of Theoretical and Computational Chemistry 2015; 14 (1): 1550004. doi: 10.1142/s0219633615500042
24. Zhang MX, Yan B.F, Li WZ, Li QZ, Cheng JB. The insertion and H_2 elimination reactions of $H_2GeFMgF$ germylenoid with RH (R = Cl, SH, PH_2). Russian Journal of Physical Chemistry A 2017; 91 (9): 1660-1668. doi: 10.1134/S0036024417090205
25. Zhang GX, Qi YH, Xu CJ. Theoretical study on the substitution reactions of the germylenoid H_2GeLiF with SiH_3X (X = F, Cl, Br). Journal of Molecular Modeling 2016; 22 (6): 130. doi: 10.1007/s00894-016-2997-x
26. Lu XH, Han JF, Lian ZX. Ab initio study of the mechanism of the formation of a bis-heterocyclic compound containing Si and Ge by reaction of germylene silylene (H_2Ge=Si:) and ethene. Journal of the Serbian Chemical Society 2011; 76 (10): 1395-1401. doi: 10.2298/JSC100921124L
27. Lu XH, Lian ZX, Li YQ, Wang ZN. Ab initio study of mechanism of forming bis-

heterocyclic compound with Si and Ge between dimethylsilylene germylidene (Me_2Si=Ge:) and ethene. Structural Chemistry 2012; 23 (3): 809-813. doi: 10.1007/s11224-011-9929-2

28. Bao WJ, Li YQ, Lu XH. Density functional theory study of mechanism of forming a spiro-Ge-heterocyclic ring compound from H_2Ge=Ge: and ethene. Structural Chemistry 2013; 24 (5): 1615-1619. doi: 10.1007/s11224-013-0199-z
29. Lu XH, Ji H. Ab initio study of mechanism of forming a spiro-ge-heterocyclic ring compound. Structural Chemistry 2013; 24 (1): 159-164. doi: 10.1007/s11224-012-0046-7
30. Liu DT, Lian ZX, Lu XH. Ab initio study of the reaction between silylene germylidene (H_2Si=Ge:) and ethene to form a bis-heterocyclic compound containing Si and Ge. Progress in Reaction Kinetics and Mechanism 2013; 38 (2): 197-203. doi: 10.3184/146867813X13632857557617
31. Lu XH, Lian ZX, Li YQ. Ab initio study of the formation of bis-heterocyclic compound involving Si and Ge from dichlorosilylene germylidene (Cl_2Si=Ge:) and ethene. Russian Journal of Physical Chemistry A 2012; 86 (12): 1869-1874. doi: 10.1134/S0036024412120278
32. Zhang XL, Zhang MX, Yan BF, Li WZ. A spiro-Ge-heterocyclic compound formation via germylenoid and formaldehyde: a theoretical study. Russian Journal of Physical Chemistry A 2020; 94 (10): 2084-2090. doi: 10.1134/S0036024420100349
33. Frisch MJ, Trucks GW, Schlegel HB, Scuseria GE, Robb MA, et al. Gaussian 09, revision A02. Gaussian Inc, Wallinford, CT, 2009.

34. Zhao Y, Truhlar DG. The M06 suite of density functionals for main group thermochemistry, thermochemical kinetics, noncovalent interactions, excited states, and transition elements: two new functionals and systematic testing of four M06-class functionals and 12 other functionals. Theoretical Chemistry Accounts 2008; 120 (1): 215-241. doi: 10.1007/s00214-007-0310-x
35. Zhao Y, Truhlar DG. Density functionals with broad applicability in chemistry. Accounts of Chemical Research 2008; 41 (2): 157-167. doi: 10.1021/ar700111a
36. Hehre WJ, Radom L, Schleyer PvR, Pople JA. Ab Initio Molecular Orbital Theory 1986, Wiley, New York.
37. Gonzales C, Schlegel HB. Improved algorithms for reaction path following: Higher-order implicit algorithms. The Journal of Chemical Physics 1991; 95 (8): 5853-5860. doi.org/10.1063/1.461606
38. Gauss J, Cremer D. Analytical evaluation of energy gradients in quadratic configuration interaction theory. Chemical Physics Letters 1988; 150 (3-4): 280-286. doi: 10.1016/0009-2614(88)80042-3
39. Salter EA, Trucks GW, Bartlett RJ. Analytic energy derivatives in many-body methods. I. First derivatives. The Journal of Chemical Physics 1989; 90 (3): 1752-1766. doi: 10.1063/1.456069

Figure captions:

Figure 1. The geometries of the stationary points along the potential energy surfaces of the addition reaction of $H_2GeLiCl$ and acetone optimized at the M06-2X /6-311+G (d, p) level (Bond lengths are given in nm and angles in degrees).

Figure 2. The potential energy surface profile of step 1 (the relative energies are given in kJ/mol).

Figure 3. The geometries of the stationary points along the potential energy surfaces of the addition reaction of *c*-$H_2GeOC(CH_3)_2$ and acetone optimized at the M06-2X /6-311+G (d, p) level (Bond

lengths are given in nm and angles in degrees).

Figure 4. The potential energy surface profile of path I and path II (the relative energies are given in kJ/mol).

Figure 5. The calculated IRC results of three transition states.

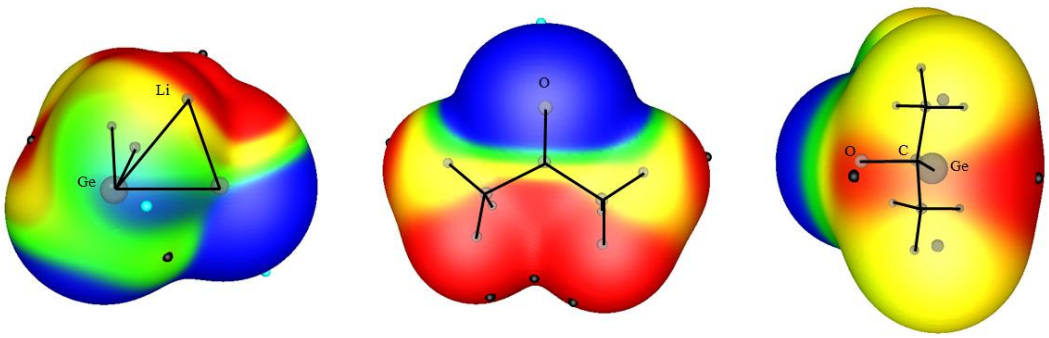

R1 R2 P

Scheme 1 The molecular electrostatic potentials for the reactants (R1, R2, and P) calculated at M06-

2X/BSI level. (Color ranges are: red, greater than 0.03; yellow, between 0.03 and 0; green, between 0 and -0.01; bule, less than -0.01, in eV.)

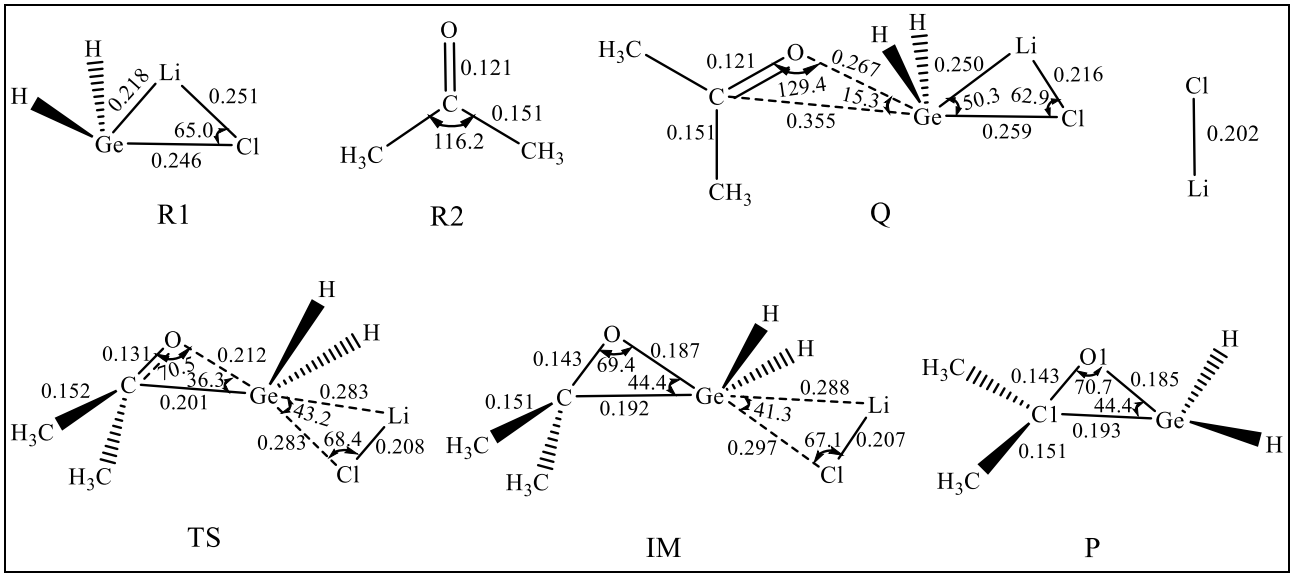

(**Figure 1**)

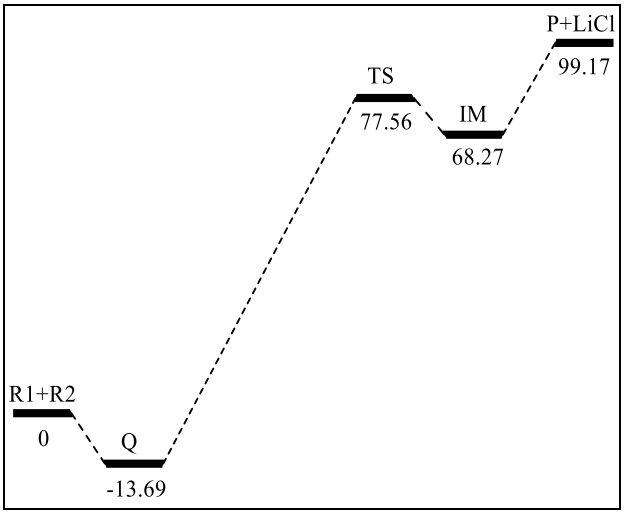

(Figure 2)

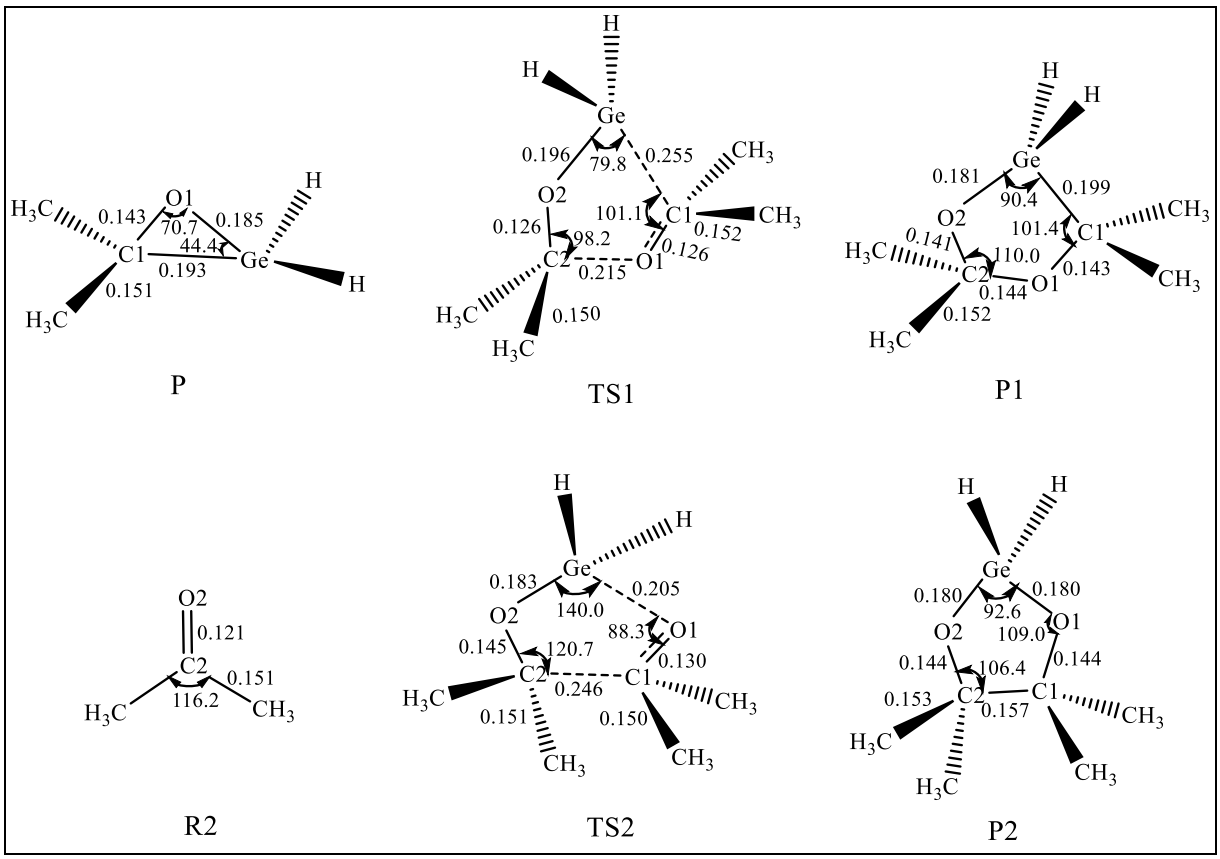

(Figure 3)

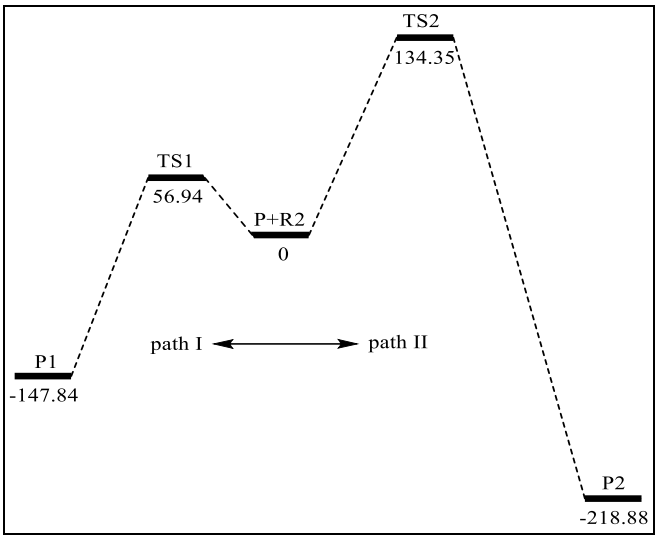

(Figure 4)

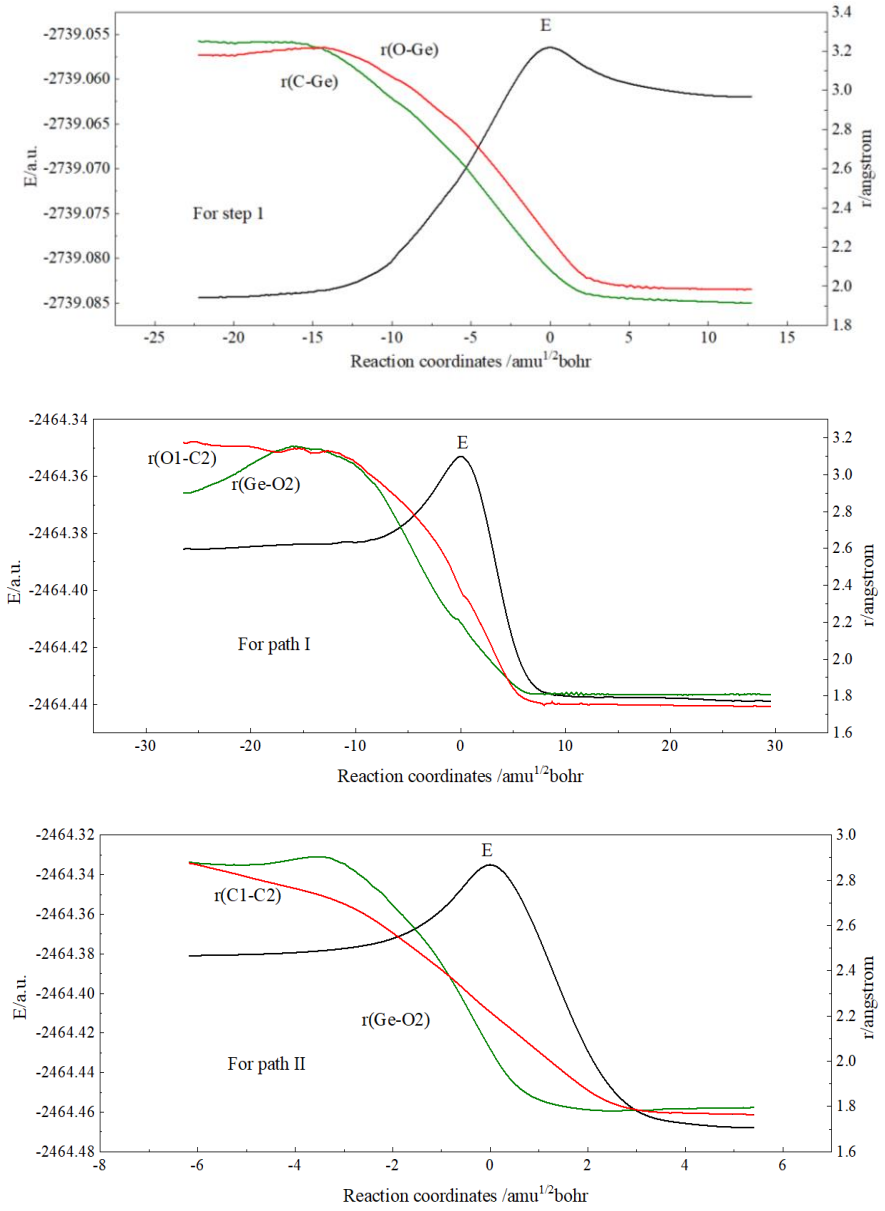
E
r(O-Ge)
r(C-Ge)
For step 1
E/a.u.
r/angstrom
Reaction coordinates /amu^1/2bohr
r(O1-C2)
r(Ge-O2)
For path I
r(C1-C2)
r(Ge-O2)
For path II

(Figure 5)

Supporting information

The structure coordinates of reactants, intermediates, transition states and products:

R1:

Ge	-2.56829	-0.28241	-0.00284
H	-2.78369	0.89251	1.12108
H	-2.78763	0.90659	-1.11107
Li	-4.23708	1.59101	0.01196
Cl	-5.0275	-0.44301	0.00049

R2:

C	2.50731	-0.37278	0.60534
O	1.54757	0.29175	0.30668
C	2.3953	-1.85413	0.89342
H	2.7478	-2.06328	1.90679
H	1.36199	-2.17702	0.78596
H	3.03472	-2.41561	0.20729
C	3.89238	0.22709	0.71334
H	4.28682	0.07265	1.72104
H	4.57088	-0.27759	0.02064
H	3.85582	1.29078	0.48805

Q:

Ge	-0.84749	-0.46504	0.0182
H	-0.75031	0.8763	0.93765
H	-0.79836	0.5103	-1.28457
Li	-1.94153	1.76091	-0.32943
C	2.70521	-0.43519	0.04558
O	1.71284	0.23225	-0.14528
C	4.08214	0.15143	-0.14277
H	4.73268	-0.11611	0.69264
H	4.52445	-0.27635	-1.0474
H	4.01855	1.23231	-0.24837
C	2.63324	-1.87709	0.47914
H	3.33185	-2.48565	-0.09904
H	2.93975	-1.94048	1.5276
H	1.61797	-2.25726	0.37951
Cl	-3.35742	0.15328	-0.03065

TS:

Ge	-0.28391	-0.30278	0.07138
H	-0.7351	-0.52581	-1.43903
H	-0.59787	-1.59492	0.83841
Li	-2.5419	-0.23429	-1.63119
C	1.72312	0.25602	-0.00533
O	1.64948	-0.96084	-0.4839
Cl	-3.02224	0.36362	0.30496
C	2.32919	0.436	1.37158
H	3.41852	0.38519	1.25455
H	2.06628	1.39989	1.80745
H	2.02546	-0.37135	2.03752
C	2.00111	1.38179	-0.97981
H	1.73052	2.35288	-0.56511
H	3.07819	1.37311	-1.18573
H	1.47894	1.21564	-1.92178

IM:

Ge	0.13164	0.34786	-0.13985
H	-0.55325	0.72195	1.22229
H	-0.09623	1.35683	-1.25292
Li	-2.2985	-0.04348	1.35567
C	1.43682	-1.05163	-0.05039
O	1.94242	0.2336	0.32457
Cl	-2.67869	-0.46143	-0.63336
C	2.04589	-1.59632	-1.32161
H	3.08475	-1.87996	-1.11644
H	1.50407	-2.47651	-1.67312
H	2.05476	-0.84549	-2.11279
C	1.40887	-2.04325	1.09046
H	0.83067	-2.93194	0.82853
H	2.43729	-2.34825	1.31623
H	0.99435	-1.59505	1.99576

LiCl:

Li	-3.85526	-1.28196	0.15847
Cl	-2.20558	-1.69782	-0.93094

P:

Ge	-0.51681	0.05007	0.00228
H	-1.26589	0.3489	1.3034
H	-1.27687	0.33029	-1.29664
C	1.28974	-0.6225	-0.00097

O	1.17372	0.80248	-0.01028
C	1.90178	-1.16101	1.27092
H	1.81037	-2.24763	1.32258
H	2.9658	-0.89824	1.28733
H	1.43533	-0.72135	2.1537
C	1.89037	-1.1783	-1.2709
H	2.95423	-0.91604	-1.30032
H	1.79832	-2.26548	-1.30735
H	1.4161	-0.7503	-2.15526

TS1:

Ge	-0.70694	-1.33075	-0.08446
H	-0.95848	-2.29472	-1.29068
H	-0.29844	-2.34449	1.04574
C	1.76486	0.07342	-0.04701
O	1.07275	-0.76459	-0.67773
C	-0.95839	1.20527	0.07982
O	0.23587	1.5563	0.27399
C	2.69522	0.9483	-0.81943
H	2.38818	0.98949	-1.86239
H	2.69543	1.94723	-0.38482
H	3.70703	0.53478	-0.75059
C	1.96295	-0.06431	1.43051
H	2.69793	-0.86179	1.59181
H	2.33201	0.86467	1.85934
H	1.03346	-0.34857	1.92268
C	-1.53259	1.41457	-1.31337
H	-2.49153	0.9144	-1.45055
H	-1.67228	2.49507	-1.44514
H	-0.82468	1.07352	-2.06981
C	-1.9361	1.35947	1.23366
H	-2.15024	2.43081	1.33377
H	-2.87238	0.83015	1.05967
H	-1.4839	1.01718	2.16396

P1:

Ge	0.88674	-0.02142	0.11379
H	1.67374	-0.33239	1.40507
H	1.80997	0.0172	-1.11503
C	-1.65884	-0.73743	0.22796
O	-0.40761	-1.25096	-0.17448
C	-0.48907	1.41459	0.26209
O	-1.69302	0.6808	0.0054
C	-0.37237	2.44679	-0.85503

H	-1.24619	3.10508	-0.83179
H	0.52489	3.05891	-0.73279
H	-0.33828	1.96385	-1.83346
C	-0.5531	2.10935	1.62063
H	0.34474	2.71128	1.78609
H	-1.42227	2.77397	1.64214
H	-0.64569	1.4054	2.4482
C	-1.89654	-1.06138	1.70109
H	-2.81251	-0.58355	2.0526
H	-1.97907	-2.14237	1.82426
H	-1.06061	-0.71879	2.31495
C	-2.73591	-1.31956	-0.66498
H	-2.74947	-2.40536	-0.56324
H	-3.71158	-0.91613	-0.38933
H	-2.5169	-1.05726	-1.69975

TS2:

Ge	0.68396	-1.10731	0.02721
H	0.58035	-1.9134	-1.26697
H	1.05877	-1.71586	1.37684
C	0.72405	0.98365	-0.04446
O	1.92038	0.19944	-0.30405
C	-1.48764	-0.09404	0.051
O	-1.30995	-1.30662	0.47915
C	-1.93054	0.06797	-1.38294
H	-2.95593	-0.32148	-1.40058
H	-1.94745	1.10311	-1.71394
H	-1.33971	-0.54049	-2.06654
C	-2.05019	0.89951	1.02385
H	-1.58753	0.79366	2.00311
H	-1.98008	1.92612	0.66667
H	-3.11139	0.63703	1.12129
C	0.49547	1.93061	-1.19704
H	-0.37364	2.57572	-1.0429
H	1.38496	2.56806	-1.27395
H	0.39034	1.39974	-2.14432
C	0.88985	1.7115	1.27763
H	1.84541	2.24681	1.2292
H	0.09822	2.43887	1.46224
H	0.94201	1.02692	2.12797

P2:

Ge	-1.65214	0.00018	-0.00014
H	-2.49414	-0.55066	1.16046

H	-2.49416	0.5511	-1.16068
C	0.86894	0.78242	0.07591
O	-0.41121	1.13601	0.62786
C	0.86872	-0.78264	-0.07579
O	-0.41136	-1.1358	-0.62817
C	1.00967	-1.47691	1.2795
H	0.78297	-2.53656	1.15089
H	2.02269	-1.38313	1.67616
H	0.31468	-1.0573	2.01238
C	1.92721	-1.29035	-1.04384
H	2.92502	-0.96276	-0.74027
H	1.91077	-2.38167	-1.05491
H	1.72614	-0.93648	-2.0548
C	1.92728	1.28978	1.04431
H	2.92509	0.96189	0.74104
H	1.91117	2.3811	1.05539
H	1.72579	0.93595	2.0552
C	1.01054	1.47664	-1.27933
H	0.78416	2.53636	-1.1508
H	2.02365	1.38251	-1.67569
H	0.31563	1.05724	-2.01241